Proceedings of the 11th ICPMG 2026
11th International Conference on Physical Modelling in Geotechnics
8-12 June 2026, Zurich, Switzerland

Centrifuge modelling of piled rafts under generalised loads

F. Potini
Università degli Studi Niccolò Cusano, Roma, Italia, francesco.potini@unicusano.it

G.M.B. Viggiani
University of Cambridge, Cambridge, UK, gv278@cam.ac.uk

R. Conti
Università degli Studi di Roma "Tor Vergata", Roma, Italia, riccardo.conti@uniroma2.it

ABSTRACT: Recent theoretical, numerical, and experimental studies have contributed to a better understanding of the ultimate behaviour of pile groups under combined vertical, moment, and horizontal loads. However, the interaction mechanisms occurring at failure within the piles-raft-soil system are still not fully understood and, therefore, the design of piled rafts is typically carried out neglecting the contribution of the connecting raft to the overall capacity of the foundation. This work presents the results of centrifuge tests on small-scale models of piled rafts embedded in clay and subjected to combined loads in undrained conditions, carried out to investigate the main factors governing their behaviour at failure. The tests were carried out on 3×3 piled foundations, consisting of miniature reinforced concrete (RC) piles rigidly connected to a Perspex raft embedded into a uniform layer of Speswhite Kaolin. The RC piles were made of a mortar of cement, water and sand, reinforced using a stainless-steel cage consisting of longitudinal bars and a confining helicoidal wire. Laboratory tests were performed to characterise the structural resistance of the miniature RC piles under combined axial and bending loads using a modified four bending point apparatus. Centrifuge tests were carried out at 100g, each including different model foundations, with different loading conditions. The vertical load was applied as a dead load, and the foundations were brought to failure under displacement control applying a horizontal displacement with different eccentricities. It was observed that the contribution of the raft expands significantly the failure domain of the foundation with respect to the case of the pile group.

1 INTRODUCTION

The design of piled foundations for modern transport infrastructure is increasingly influenced by the need to balance structural safety with evolving sustainability targets. In seismic regions, horizontal actions tend to dominate the design of the foundation system inducing multiaxial loading conditions characterised by complex soil–raft–piles interaction.

Considerable effort has been devoted to developing alternatives to the overly conservative design procedures adopted in practice, which fail to account properly for the coupling among vertical (V), horizontal (H) and moment (M) actions. Within this context, interaction domains at failure provide a valuable framework for implementing capacity-based design strategies for pile groups (Di Laora et al., 2019; Gorini & Callisto, 2022; Potini et al., 2023; Sakellariadis & Anastasopoulos, 2024a,b; Potini et al., 2025; Di Laora et al., 2025).

Although theoretical and numerical modelling allow for a systematic and parametric investigation of the key factors governing the behaviour of piled-raft foundations, physical modelling remains essential to capture phenomena that may be difficult to model, such as the nonlinear load sharing between piles and raft and the emergence of failure mechanisms without imposing predefined constitutive assumptions.

Early experimental evidence on the bearing capacity of pile groups under combined loading were provided by Meyerhof and Ranjan (1973), who considered a rigid behaviour of the pile group. Experimental 1g loading apparatus for tracing the three-dimensional V-H-M failure envelopes of shallow and spud can foundations were developed by Gottardi (1992) and Martin (1994), respectively.

The first experimental insights on the response of piled rafts were provided by Cooke (1986), who conducted 1g vertical loading tests on small-scale piled raft models embedded in remoulded London Clay in undrained conditions. Through a combination of physical modelling and theoretical interpretation, Cooke demonstrated that the ultimate failure mechanisms of a piled raft under pure vertical load are confined between two bounding modes: (i) piles punching, and (ii) block failure, providing a lower bound and an upper bound for the capacity of the piled raft, respectively.

Moving to more recent literature, several centrifuge experimental campaigns have been carried out, some aimed at understanding the failure behaviour of piled foundations under complex loading conditions, and others focused on clarifying the contribution of the connecting raft to the overall foundation capacity. de Sanctis et al. (2021) and Iovino et al. (2023) investigated the failure mechanisms of annular-shaped pile groups subjected to combined loading in clayey and sandy soils, respectively. The former examined the foundations response under monotonic V-M loading only, whereas the latter also explored the behaviour under V-H loading, considering both monotonic and cyclic load paths.

In this context, a versatile combined loading apparatus capable of imposing arbitrary displacement paths, including settlement, lateral translation and rotation, was developed at ETH Zurich and deployed in the drum centrifuge to investigate the behaviour of piled foundations under fully controlled V-H-M loading conditions (Sakellariadis & Anastasopoulos, 2024a; Sakellariadis et al., 2023, 2025).

Although notable experimental research efforts have been devoted to understanding the contribution of the raft to the overall resistance of the foundation (Conte et al., 2003; Katsanevaki et al., 2022; Katsanevaki, 2023; Marveggio et al., 2024), this aspect remains only partially understood and therefore this is often neglected in engineering applications. Potini et al. (2026) showed that the connecting raft plays a significant role in the capacity of piled rafts under combined loading, based on advanced Finite Element (FE) analyses and Limit Analysis theory. The Authors provided four simplified approaches for evaluating the interaction domain at failure of a piled raft subjected to vertical eccentric loads.

To provide new insights into the failure behaviour of piled-raft foundations, this work presents some preliminary results of an experimental campaign including 100g static centrifuge tests carried out at the Schofield Centre of the University of Cambridge. A reference square 3×3 piled raft, with spacing $s = 4d$, embedded in Speswhite Kaolin was brought to failure under different V-H-M loading conditions (Fig. 1).

The moment capacity of piled rafts (M_u) arises from three main mechanisms (Sakellariadis & Anastasopoulos, 2024a): the distribution of axial forces among the piles (M_{ax}), the development of plastic hinges at the pile–raft connections (M_b) and the soil resistance mobilised under the connecting raft (M_R). To ensure that these three contributions are properly represented in the physical model, miniature reinforced concrete (RC) piles were constructed and rigidly connected to the raft, allowing the axial force in the individual piles to be measured.

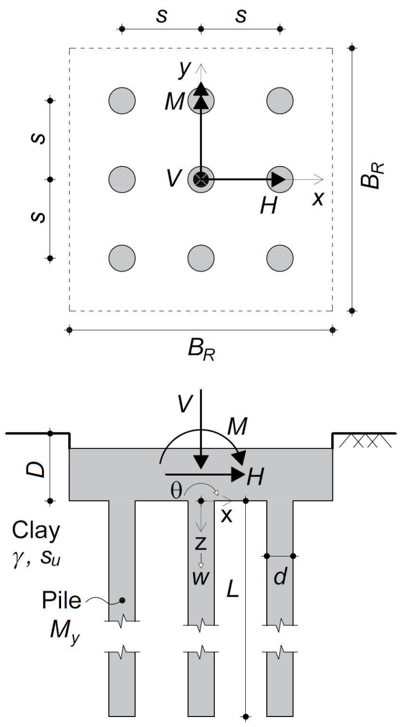

Figure 1. Problem layout.

2 MODEL PREPARATION AND SETUP

2.1 Miniature RC piles

Miniature RC piles were previously developed by Katsanevaki (2023). In that study, the reinforcement cage was made using a galvanized steel wire mesh with a wire diameter of 0.18 mm and a cell size of 1.2 mm. The mesh was rolled around a brass rod to obtain the required circular geometry and then it was fixed minimising overlap, resulting in a reinforcement cage with an external diameter of approximately 6.5 mm. The model piles were casted using a cylindrical mould with an internal diameter (d) of 10 mm and a length (L) of 200 mm. A cement mortar was poured into the mould, and the reinforcement cage was then inserted. The mortar consisted solely of water and cement, with a water–cement ratio of 0.5; no sand was added to the mortar to ensure a highly fluid and workable mix, which was necessary due to the casting procedure and the flexibility of the miniature reinforcement cages (Katsanevaki & Viggiani, 2022).

In this study, a different procedure was employed to make the miniature RC piles, introducing substantial technological refinements to enhance both the geometrical accuracy of the model piles and the reliability and repeatability of their structural response. Stainless-steel wires were used to model the reinforcement cage of the piles, both for the longitudinal rebars and the helicoidal confinement. The longitudinal reinforcement consisted of six bars, while the helicoidal confinement had a pitch of 10 mm; the corresponding wire diameters were 0.6 mm and 0.4 mm, respectively. The longitudinal bars were positioned along an aluminium guide featuring longitudinal grooves, and were subsequently wrapped with the helical confinement, which was fixed to the bars using a high-strength epoxy adhesive. After allowing sufficient curing time for the adhesive, the completed cages were carefully removed from the guide. The reinforcement was designed to achieve a reinforcement ratio of approximately 2 %, corresponding to a prototype pile with $d = 1$ m and a 32ϕ26 reinforcement (Fig. 2).

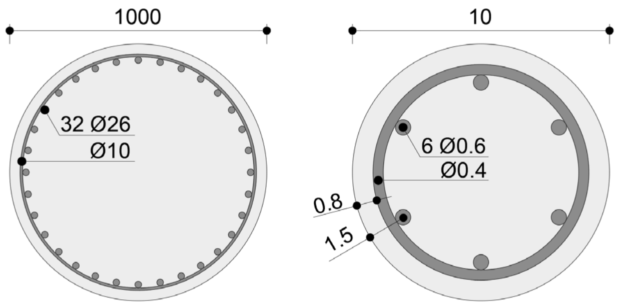

(a) (b)

Figure 2. RC piles cross-section: (a) prototype and (b) model; dimensions are given in mm.

A sand-cement mortar was used to model the concrete of the miniature piles. The mix was prepared using water, cement and Leighton Buzzard Sand (fraction E), with both water-cement and sand-cement ratios of 0.5 by weight. The introduction of sand into the mortar was made possible by the high stiffness of the reinforcement cages: the cages were sufficiently rigid to be inserted into the mould after it was completely filled with the fresh mortar (Fig. 3.), without undergoing distortion or loss of geometric accuracy (Katsanevaki, 2023).

To ensure a rigid connection between the piles and the raft, aluminium caps equipped with an M3 threaded bar were installed at the pile heads. The threaded bar was sized and positioned so as not to extend down to the portion of the pile where the plastic hinge was expected to develop. Figure 4 provides a schematic representation of the piles longitudinal section. To maximise the adhesion at the pile–soil interface, the external surface of each pile was coated with a mixture of water-resistant epoxy adhesive and Leighton Buzzard Sand (fraction E). The thickness of the sand–epoxy layer surrounding the pile is negligible compared to the pile diameter and, therefore, it does not alter the overall cross-sectional dimensions of the pile. Model piles were designed to have an effective free length of $L = 200$ mm. However, to provide a rigid head restraint and prevent pile rotation under combined loading, the upper 20 mm of each pile was inserted within the connecting raft. Therefore, the piles were manufactured with a total length of 220 mm.

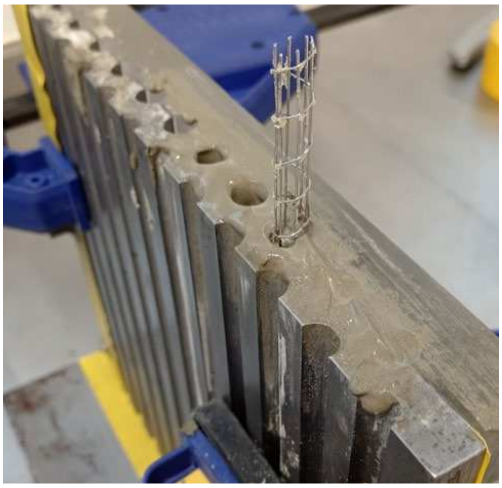

Figure 3. Mould adopted for the RC piles casting.

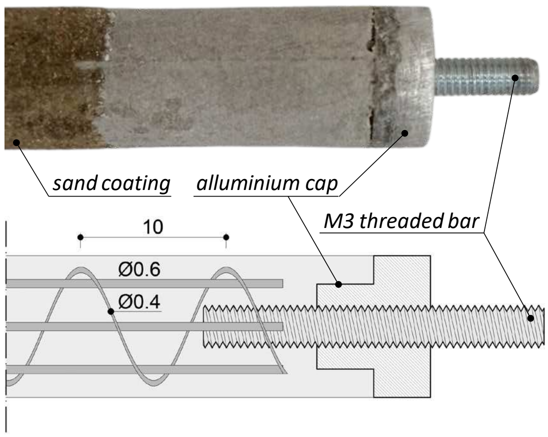

Figure 4. RC piles longitudinal section; dimensions are given in mm.

2.2 Connecting raft and instrumentation

As shown in Figure 5, the connecting raft was assembled from horizontal and vertical Perspex plates rigidly joined together using M3 threaded bars. Following Katsanevaki (2023), the Perspex plates were assembled in a sandwich configuration to provide sufficient space for the installation of load cells (LCs) at the head of some piles, allowing to measure the axial force distribution among the piles during the loading phase. LCs had a capacity of 200 N (model FLAE/Forsentek) both in compression and tension. The holes in the bottom plate were larger than the pile diameter to accommodate PTFE sleeves between the pile surface and the hole walls. These sleeves were used to minimise axial friction within the pile–raft connection and to ensure that the entire axial load carried by the pile is transmitted to the load cell. At the head of the piles that were not instrumented with load cells, metallic connectors of the same dimensions as the load cells were installed to ensure identical stiffness throughout the connecting raft. To reproduce a realistic interface condition between the raft and the soil, the bottom surface of the connecting raft was also roughened by applying a sand layer bonded with water-resistant epoxy resin.

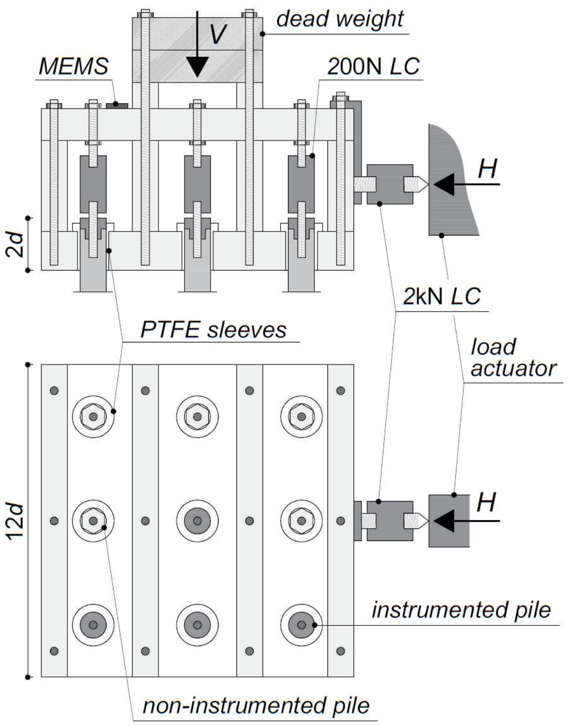

Figure 5. Lateral and planar representation of the instrumented connecting raft.

Figure 6 shows the assembled piled raft model. To measure the rotations of the foundation during the tests, triaxial Micro-Electro-Mechanical-Systems (MEMS) sensors were attached to the top plate of the connecting raft. The total vertical load (*V*) applied to the foundation system during the test was kept constant and was imposed by placing a dead weight consisting of brass plates, which were secured to the connecting raft. The horizontal eccentric load (*H*) was applied using a displacement-controlled actuator and measured by a 2 kN LC (model FSSH/Forsentek). Different loading conditions were investigated by varying both the vertical position of the applied horizontal load and the amount of vertical dead weight.

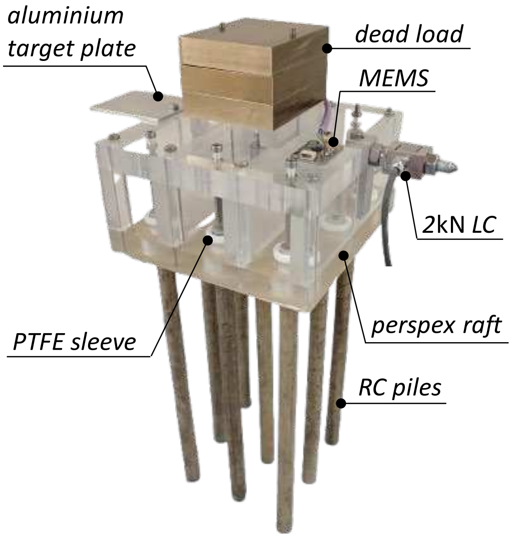

Figure 6. Assembled 3×3 piled raft model.

2.3 Soil preparation and models installation

2.3.1 Soil consolidation

The clay layer was prepared within a cylindrical container with an internal diameter of 850 mm. Figure 7 shows schematically the apparatus used to consolidate the clay at 1*g*.

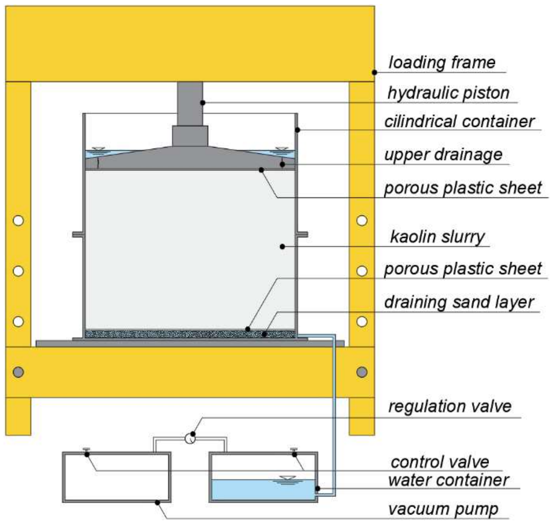

Figure 7. Schematics of the consolidation rig.

A 30 mm draining layer consisting of dense Fraction-B Leighton Buzzard sand (D_{50} = 0.80 mm) was first placed at the bottom of the container. A porous plastic sheet and a filter paper were positioned above the sand to prevent the migration of clay particles into the draining layer. The clay layer was produced from a slurry obtained by mixing Speswhite kaolin powder with de-aired water at a water content *w*/c = 1.2. The slurry was then poured into the container and subjected to one-dimensional consolidation at 1*g*, where both upward and downward drainage were allowed, using a computer-controlled hydraulic press (Madabhushi, 2017). The vertical load was incrementally applied with a piston at the soil surface until reaching a maximum effective stress of 160 kPa. At the same time, suction was incrementally applied at the bottom of the soil model until reaching a maximum value of 80 kPa. Final consolidation occurred in-flight at 100*g* in the centrifuge.

2.3.2 Piled raft installation

At the end of the 1*g* consolidation stage, the soil surface was trimmed to obtain the target clay thickness of approximately 270 mm. The clay surface was then carefully excavated to create a shallow recess for the partially embedment of the connecting raft. Moreover, boreholes were formed to accommodate the model piles. To ensure full contact between the piles and the soil, while limiting disturbance to the surrounding soil, the boreholes were drilled down to a depth of 190 mm using a 9 mm bit, slightly smaller than the 10 mm pile diameter. Given the pile length of 200 mm, this procedure ensured that the pile tips would come into direct contact with the underlying soil, to ensure full end-bearing engagement and avoiding unwanted gaps beneath the pile base. After completing the excavation and preparing the boreholes, the fully assembled foundation model was carefully pushed into position. Particular attention was paid to maintaining verticality and minimising soil disturbance during installation, so as to preserve the intended pile–soil contact conditions and ensure repeatability across the test series. Given the dimensions of the cylindrical container, a maximum of four foundation systems could be placed and tested within each experimental run.

3 PILES STRUCTURAL BEHAVIOUR

To characterise the time-dependent mechanical properties of the mortar used to cast the model piles, a dedicated material testing programme was conducted. Mortar cubes with nominal dimensions of 50 mm were prepared and tested in unconfined compression at different curing times, ranging from 7 to 54 days. The results indicated that, after approximately 10 days of curing, the compressive strength stabilised at around 30 MPa, while the Young modulus settled at roughly 2100 MPa, about one order of magnitude lower than standard structural concrete. In addition to these, tensile tests were performed on the stainless-steel wires employed for the model rebars, in order to quantify their tensile strength and Young modulus.

A further investigation was conducted to characterise the structural response of the miniature piles. This programme included tests under both three-point bending (3PB) and four-point bending (4PB), as well as pure compression tests. The simple bending tests were primarily carried out on piles with a total length of 200 mm, corresponding to the geometry adopted in the centrifuge experiments. In addition, combined bending–compression tests were performed using the 4PB set-up on shortened specimens with a length of 100 mm to avoid axial buckling. Figure 8 shows the experimental setup and loading apparatus adopted for the bending-compression tests.

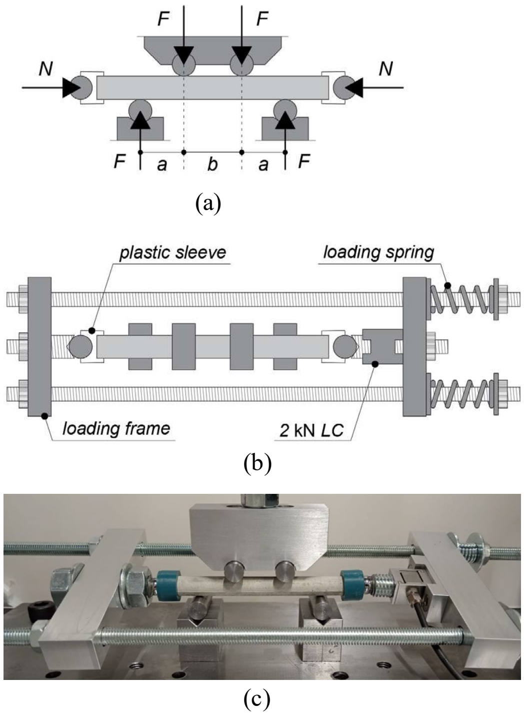

Figure 8. Schematics of the four-point bending-compression test apparatus: (a) lateral and (b) planar view; (c) photograph of the apparatus in the Instron loading frame.

As shown in Figure 8b-c, the axial load, *N*, on the pile was applied by compressing a set of springs positioned at the end of the loading frame. The force transmitted to the pile was measured using a load cell placed between the pile and the springs. The magnitude of the axial load was adjusted by tightening bolts to compress the springs accordingly. This loading apparatus was mounted on an Instron loading frame, which applied the transverse load under displacement control at a rate of 0.5 mm/min.

Figure 9 shows the results of the 3PB and 4PB tests carried out on the miniature piles of length $L = 200$ mm under pure bending conditions ($N = 0$).

For the 3PB configuration, the distance between the supports and the point of load application was $a = 127.5$ mm. In the 4PB tests, the loading scheme was defined by $a = 38.75$ mm and $b = 50$ mm (Fig. 9). A maximum vertical displacement $v/d = 1$ was imposed. The response is consistent across the tested piles: a good agreement is observed in the initial stiffness, and all specimens exhibit a markedly ductile behaviour with a large deformation capacity. The maximum yielding moment (M_{yb}) obtained for different piles varies by about 15% in the 3PB tests and by about 30% in the 4PB tests.

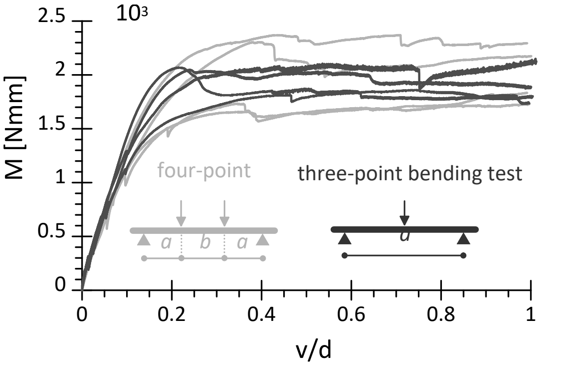

Figure 9. Moment-vertical displacement curves from three- and four-point simple bending (N = 0) tests.

The results of all structural tests are compared in Figure 10 with the theoretical *N-M* interaction domain of the reference prototype pile. To this end, the latter was scaled using a N_c^3 factor, where $N_c = 100$ is the scaling factor for lengths in the centrifuge tests. In addition to pure bending tests, Figure 10 also reports the results of the combined bending–compression tests (with $N \approx 500$ N) and of pure compression tests carried out on pile specimens with a $L = 4d$. The theoretical interaction domain of the prototype pile was obtained from a section analysis carried out using the constitutive relationships for steel and concrete reported by Potini & Conti (2024).

As in the case of $N = 0$, a variability of approximately 30% is also observed for the 4PB tests performed under an axial load of $N \approx 500$ N and for the pure compression tests. For the 4PB tests, the *N-M* loading paths are also reported, highlighting a slight variation in N between the conditions of $M = 0$ and $M = M_{yb}$. The relative position of the longitudinal bars and the helicoidal reinforcement with respect to the compressed concrete in the plastic hinge region influences the variability of the results. A denser helicoidal confinement would have provided a more uniform confinement effect, thereby reducing the scatter in the measured capacities. However, the yielding moment of the model pile is observed to depend on the applied axial load, showing a qualitative trend that is in good agreement with the variability shown by the theoretical prototype domain. For the pure compression tests, the experimental results are approximately 40% lower than the theoretical values, likely due to a limited confinement provided by the reinforcement cage on the pile mortar.

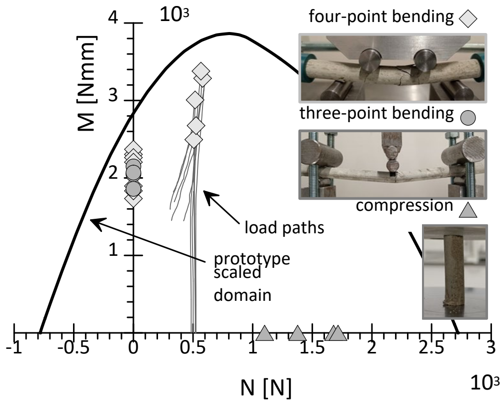

Figure 10. N-M interaction domain: experimental model pile results and theoretical prototype domain.

4 CENTRIFUGE TEST

Prior to the loading phase, the centrifuge model underwent in-flight consolidation at an acceleration of 100*g*, ensuring stabilisation of pore water pressures. Consolidation was monitored using four Pore Pressure Transducers (PPTs) installed along the soil model at equally spaced depths.

During the consolidation stage, the vertical dead load applied on the foundation systems induced settlements. These were recorded using laser displacement sensors mounted at the base of the load actuator, each targeting an aluminium plate fixed as an extension of the connecting raft top surface (Fig. 6).

After consolidation, miniature T-bar penetration tests were performed. Interpretation of the measured penetration resistance allowed to estimate the undrained shear strength profile with depth (Fig. 11).

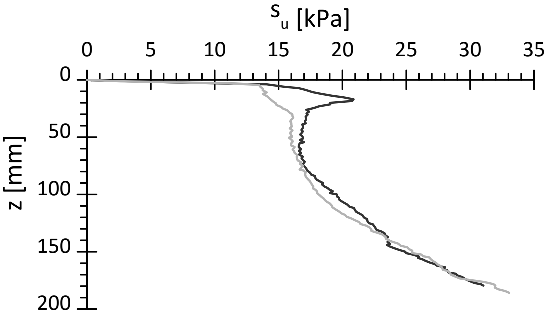

Figure 11. Undrained shear strength profiles of the soil.

The two profiles shown in Figure 11 are substantially the same, indicating a constant undrained shear strength of about 17 kPa down to a depth of about 80 mm (or about 8 m at prototype scale) and then increasing almost linearly with depth by about 0.015 kPa/mm (or 1.5 kPa/m at prototype scale).

The horizontal load on the foundation system was applied using a two-dimensional load actuator under displacement control, with a loading rate of 1 mm/s (de Sanctis et al., 2021). Figure 12 shows the horizontal load–displacement curves for one of the tested piled raft foundations, as well as for an unpiled foundation (right axis). In addition, the axial load measured on the instrumented piles within the piled raft is plotted against the horizontal displacement (left axis) and is compared with the vertical limit load of the single pile in compression. Among the various loading configurations investigated in this study, the one discussed here corresponds to the smallest horizontal load eccentricity (relative to the base of the raft), e (=M/H) = 33 mm, while for the unpiled raft e = 45 mm. With regard to the vertical load applied to the models, this was selected such that the piled raft operated at a high load level, with $V/V_{u,PR} > 0.5$, while, the applied vertical load on the unpiled raft was chosen to achieve a load ratio of $V/V_{u,R} \approx 0.5$. In particular, the vertical load V acting on the piled raft was chosen to be approximately equal to the vertical capacity of the pile group, $V_{u,P}$, thereby requiring the mobilisation of part of the raft resistance to ensure its stability.

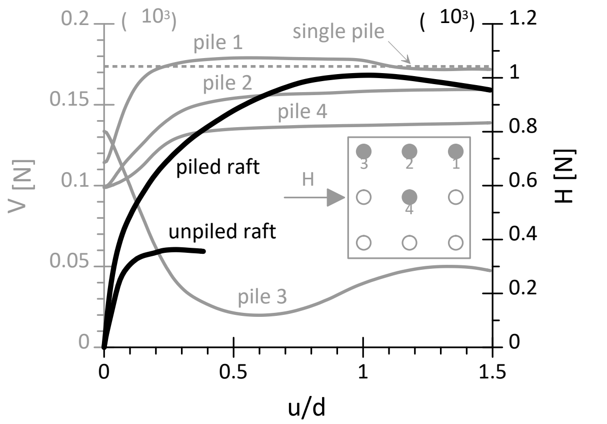

Figure 12. Load-displacement curves of a tested piled raft.

The horizontal capacity of the piled raft (≈ 1000 N) was fully mobilised for a displacement of u/d = 1, whereas the unpiled raft reached its capacity (≈ 400 N) at a horizontal displacement of u/d = 0.2. Considering that, for both systems, the rotations observed at failure were not sufficient to cause detachment of the raft base from the underlying soil, and that the exhibited rotations are comparable, this provides a reliable indication of the relative contribution of the raft and the piles to the overall horizontal resistance of the foundation system.

Regarding the distribution of vertical load among the piles, it can be observed that, before the application of horizontal displacement, the piles carried approximately the same axial force (mean value ≈ 120 N). Due to the rotation of the foundation during the horizontal loading, a redistribution of axial forces among the piles occured: as expected, the leading pile (1) experienced an increase in axial load reaching its compression limit, with a more moderate load increase observed in the central piles (2 - 4), whereas the trailing pile (3) undergoes a significant reduction in axial force, though without transitioning into tension due to the high applied vertical load.

Finally, Figure 13 shows the deformed configuration of the piled raft model after extraction from the soil. The piles exhibited a long-pile failure mechanism: in addition to the plastic hinge that formed at depth, plasticity also developed at the pile head. However, due to the rotation of the raft during horizontal loading, it is not possible to clearly classify the failure mechanism as a pure double-hinge failure (Potini et al., 2025). To shed light on this aspect, further investigation is required, combining advanced numerical modelling and theoretical interpretation.

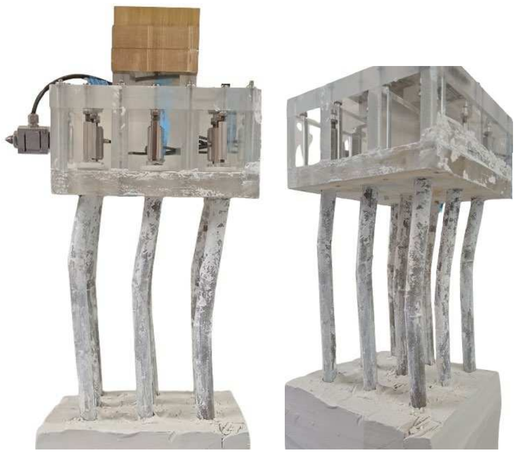

Figure 13. Deformed configuration of the piled raft model after the loading phase.

5 CONCLUSIONS

This experimental work was carried out to improve the understanding of the failure mechanisms governing piled raft foundations, where complex interaction phenomena between the raft, the piles and the surrounding soil make it challenging to clearly identify and quantify the individual resistance components contributing to the overall capacity of the foundation. The experimental results demonstrate that the raft, often neglected or treated conservatively in design practice, can provide a significant contribution to the capacity of the foundation under combined loading.

The results of this experimental campaign provide a valuable benchmark for the validation of numerical models and theoretical methods to be employed in the design of piled foundations and in the retrofitting of existing infrastructures.

ACKNOWLEDGEMENTS

The research presented in this article was funded by Regione Lazio (Italy) and Italferr S.p.A. within the programme POR-FSE 2014-2020 (Grant Agreement no. F83C22000770005). The authors wish to thank the technicians at the NRFIS Laboratories and the Schofield Centre for their support. The first author also gratefully acknowledges Mr. Nicolas Lee for his valuable advice and assistance during the preparation of the centrifuge tests.

REFERENCES

Conte, G., Mandolini, A., & Randolph, M. (2003). Centrifuge modelling to investigate the performance of piled rafts. In *Centrifuge modelling to investigate the performance of piled rafts* (pp. 359-366). Millpress.

Cooke, R.W. (1986). Piled raft foundations on stiff clays - a contribution to design philosophy. *Geotechnique*, Vol. 36 No. 2 pp. 169–203.

de Sanctis, L., Di Laora, R., Garala, T. K., Madabhushi, S. P. G., Viggiani, G. M. B., & Fargnoli, P. (2021). Centrifuge modelling of the behaviour of pile groups under vertical eccentric load. *Soils and Foundations*, 61(2), 465-479.

Di Laora, R., de Sanctis, L., Aversa, S. (2019). Bearing capacity of pile groups under vertical eccentric load. *Acta Geotechnica*, 14(1) pp. 193-205.

Di Laora, R., Cesaro, R., Iodice, C., Iovino, M., & de Sanctis, L. (2025). A closed form solution for the generalised failure envelope of a pile group. *Soil Dynamics and Earthquake Engineering*, 199, 109623.

Gorini, D. N., & Callisto, L. (2022). Generalised ultimate loads for pile groups. *Acta Geotechnica*, 17(6), 2495-2516.

Gottardi, G. (1992). *Modellazione del comportamento di fondazioni superficiali su sabbia soggette a diverse condizioni di carico* (Doctoral dissertation, University of Padua, Italy).

Iovino, M., Iodice, C., Alagha, A., Viggiani, G.M.B. (2023). Centrifuge Experiments Dealing with Monotonic and Cyclic Loads on Pile Foundations in Sand. In: *Geotechnical Engineering in the Digital and Technological Innovation Era*. CNRIG 2023. Springer Series in Geomechanics and Geoengineering. Springer, Cham. https://doi.org/10.1007/978-3-031-34761-0_81.

Katsanevaki, Z. (2023). *Numerical and physical modelling of piled rafts on soft clay under combined loading* (Doctoral dissertation, University of Cambridge, UK).

Katsanevaki, Z., & Viggiani, G.M.B. (2022). Modelling small RC piles for geotechnical centrifuge testing. *Proceedings of the 10th International Conference on Physical Modelling in Geotechnics* (ICPMG2022), Korea.

Katsanevaki, Z., Viggiani, G.M.B., & Madabhushi, G.S.P. (2022). Physical & numerical modelling of piled rafts under lateral loading. *Proceedings of the 10th International Conference on Physical Modelling in Geotechnics* (ICPMG2022), Korea.

Madabhushi, G.S.P. (2017). *Centrifuge Modelling for Civil Engineers*. London: CRC Press.

Martin, C. M. (1994). *Physical and numerical modelling of offshore foundations under combined loads* (Doctoral dissertation, Oxford University, UK).

Marveggio, P., Corigliano, M., Ovalle-Villamil, W., Flessati, L., & Cabrera, M. (2024). Physical modelling of piled foundation under combined loading: insights on the piles-raft-soil coupling. *Proceedings of the 5th European Conference on Physical Modelling in Geotechnics*, Delft, the Netherlands.

Meyerhof G.G., Ranjan G. (1973). The bearing capacity of rigid piles under inclined loads in sand. iii: pile groups. *Can. Geotech. J.*, 10:428–438.

Potini, F., Gorini, D.N., Conti, R. (2023). Rigorous lower and upper bounds for the generalised failure loads of pile groups. *Géotechnique Letters*, 13(2):1–7.

Potini, F., & Conti, R. (2024). Horizontal Bearing Capacity of RC Piles in Cohesive Soil: Numerical and Theoretical Modelling. *Computers and Geotechnics*, 175, 106638.

Potini, F., Viggiani, G.M.B., Conti, R. (2025). Interaction domains of pile groups in cohesive soils under generalised loads. *Géotechnique*, Vol. 75 No. 11 pp. 1375–1387, doi.org/10.1680/jgeot.24.01210.

Potini, F., Viggiani, G.M.B., Rotunno, A.F., Berardi, L., Conti, R. (2026). Interaction domains of piled raft foundations in cohesive soils under vertical-eccentric loads. *Géotechnique*, doi.org/10.1680/jgeot.25.00539.

Sakellariadis, L., & Anastasopoulos, I. (2024a). On the Mechanisms Governing the Response of Pile Groups Under Combined VHM Loading. *Géotechnique* 74, No. 9, 840–861, doi.org/10.1680/jgeot.21.00236.

Sakellariadis, L., & Anastasopoulos, I. (2024b). Analytical 3D failure envelopes for RC pile groups under combined loading: A generalised design approach. *Soil Dynamics and Earthquake Engineering*, 181, 108570.

Sakellariadis L, Bleiker E, Iten M, Buschor H, Kieper A, Herzog R, Marin A, Adamidis O, Anastasopoulos I (2023). Testing pile foundations at the ETH Zurich drum centrifuge: recent developments. *Int. J. Phys. Model. Geotech.*, Vol. 23 No. 5 pp. 219–247.

Sakellariadis L, Agalianos A, Alber S, Giger J, Anastasopoulos I (2025). Combined loading apparatus for monotonic and cyclic planar loading of foundations. *Int. J. Phys. Model. Geotech.*